Rare Metal Materials and Engineering
Volume 50, Issue 9, September 2021
Available online at www.rmme.ac.cn

Science Press

Cite this article as: Cui Chunjuan, Liu Wei, Deng Li, et al. Effect of Metastable Phase on Corrosion Behavior of Directionally Solidified Ni-Si Eutectic Composites[J]. Rare Metal Materials and Engineering, 2021, 50(09): 3110-3115.

ARTICLE

Effect of Metastable Phase on Corrosion Behavior of Directionally Solidified Ni-Si Eutectic Composites

Cui Chunjuan[1,4], Liu Wei[1], Deng Li[1], Wang Songyuan[1], Su Haijun[2], Lu Yu[3]

[1] School of Metallurgical Engineering, Xi'an University of Architecture and Technology, Xi'an 710055, China; [2] State Key Laboratory of Solidification Processing, Northwestern Polytechnical University, Xi'an 710072, China; [3] School of Metallurgy and Materials, University of Birmingham, Edgbaston B15 2TT, UK; [4] Shaanxi Engineering Research Center of Metallurgical, Xi'an 710055, China

Abstract: The modified Bridgman directional solidification technique was used to prepare the Ni-Si eutectic composites at solidification rate of 25 μm/s. However, the formation of metastable phase $Ni_{31}Si_{12}$ was inevitably during solidification process. Annealing treatment was conducted to reduce the number of metastable phases. Electrochemical impedance spectroscopy and potentiodynamic polarization techniques were used to analyze the corrosion resistance of Ni-Si eutectic composites in the 7wt% H_2SO_4 solution at 25 °C. The equivalent circuit was analyzed. Results show that the passivation performance and corrosion resistance behavior of Ni-Si eutectic composites are improved after annealing at 1050 °C for 4 h, which is mainly attributed to improvement of content and distribution of metastable phase $Ni_{31}Si_{12}$. The less the content of metastable phase, the stronger the corrosion resistance.

Key words: Bridgman directional solidification; Ni-Si eutectic composites; metastable phase; corrosion behavior; electrochemical

In recent years, composite materials become one of the main research directions of new materials[1,2]. After a series of phase transitions, new phases, namely metastable phase, are formed and cannot be found in the equilibrium phase diagram. Many metastable phases exist stably under certain conditions. Therefore, it is difficult to distinguish the metastable phase from stable phase. For example, Al_5Ti_3 has been regarded as a stable phase for a long time[3], while many researchers have confirmed that Al_5Ti_3 is a stable metastable phase[4,5]. Generally, solid alloys are difficult to achieve overall equilibrium, but they can exist in the form of metastable phase for a long time. Therefore, metastable phase is a very common phase structure. The influence of different metastable phases on material properties is different. During the formation of partial metastable phases, there are both negative and positive effects on material properties. Significant grain coarsening phenomenon occurs in Fe-B alloy when metastable phase Fe_3B forms[6]. Wang et al[7] achieved deep undercooling of $Cu_{40}Co_{40}Ti_{20}$ melt alloy by electromagnetic levitation technique and melt rapid quenching method, and metastable phase separation occurred. In addition, the microstructure of alloy with metastable phase improves, compared with that of the stable phase. For example, quenching-carbon partitioning-tempering (q-p-t)[8] method and aging treatment[9] are designed according to this principle. γ-MnS metastable phase prepared by hydrothermal solvent[10] displays extremely strong fluorescence at room temperature, whereas the stable phase only displays weak fluorescence. Moreover, new materials, such as martensite[11] and metastable phase Bi_2SiO_5 material[12], have been widely developed and applied. Therefore, the production, characteristics, and control of metastable phase play important roles in designing new materials. Cui et al[13] prepared Ni-Ni_3Si eutectic composites by a modified Bridgman directional solidification technique. The brittle Ni_3Si and ductile α-Ni are simultaneously precipitated. α-Ni solid solution phase is toughened at room temperature, and Ni_3Si phase is enhanced at high temperature by adjusting the solidification parameters to optimize the structure. Thus, the comprehensive mechanical properties are improved. Metastable phase $Ni_{31}Si_{12}$ has a complex hexagonal structure,

Received date: September 07, 2020
Foundation item: National Natural Science Foundation of China (51201121); Science and Technology Foundation for Selected Overseas Chinese Scholars of Shaanxi Province (2015); Key Industry Innovation Chain (Group) Project of Shaanxi Province (2019ZDLGY 04-04)
Corresponding author: Cui Chunjuan, Ph. D., Professor, College of Metallurgical Engineering, Xi'an University of Architecture and Technology, Xi'an 710055, P. R. China, Tel: 0086-29-82202923, E-mail: cuichunjuan@xauat.edu.cn

and inevitably forms during the solidification process, which results in the brittleness of composite material. Therefore, the metastable phases, especially those having a negative impact on the material properties, should be decomposed and transformed by heat treatment.

Ni-Si eutectic composites play an increasingly important role in automotive, military, and aerospace industries due to the synergistic growth between matrix phase and reinforcement phase. Most of literatures only focused on microstructure, especially the effect of solidification rate and dendrite spacing on the mechanical properties of metal alloys[13]. There are few researches about the elimination of metastable phase. Dutra[14] found that the metastable phase can be eliminated at the annealing temperature of 950 °C for 0.5 h with the low solidification rate. However, the elimination of metastable phases at high solidification rates is unclear, and the influence of metastable phase on corrosion behavior has not been well studied.

In this work, Ni-Si eutectic composites were prepared at the solidification rate of 25 μm/s through the modified Bridgman directional solidification technique. Different annealing processes were designed and conducted to transform metastable phase into stable phase. The microstructure was characterized. Then, the influence of metastable phase on corrosion behavior of Ni-Si eutectic was investigated by electrochemical measurements and immersion tests in 7wt% H_2SO_4 solution.

1 Experiment

According to the Ni-Si phase diagram, nickel (purity of 99.99%) and silicon (purity of 99.99%) were uniformly mixed to obtain the Ni-11.5wt% Si eutectic ingot in a vacuum induction melting furnace. The ingot was cut into cylindrical rods with dimension of Φ6 mm×100 mm to obtain master alloy specimens. Ni-Si eutectic composites were prepared at solidification rate of 25 μm/s through the modified Bridgman directional solidification equipment.

Different annealing processes were conducted in a high temperature vacuum tube resistance furnace. The heating temperatures were 950, 1000, and 1050 °C, and the holding durations were 2, 3, and 4 h. The specimens were furnace cooled to room temperature. After grinding and polishing, the specimens were etched by a solution of 50 mL 5vol% hydrochloric acid, 50 mL water, and 1 g ferric chloride. OLYMPUS GX51 optical electron microscopy was used to observe the morphology evolution of metastable phase before and after annealing.

Before electrochemical experiment, the Ni-Si eutectic composites were cut into the ones with the dimension of 10 mm×10 mm×5 mm by wire-cutting electric discharge machining (EDM). The surface was ground by 2000# grit and polished by 0.5 μm diamond paste to mirror-like surface. Then the specimens were connected to copper wire by single-component inorganic high-temperature conductive adhesive and inlaid with denture base resin. The test area of the specimen was 1 cm^2. Three-electrode system was used for electrochemical testing. $Ni\text{-}Ni_3Si$ eutectic specimens without heat treatment or annealing process were used as working electrodes. The platinum electrode of 10 mm×10 mm×0.1 mm was auxiliary electrodes, and the mercury-mercurous sulfate was the reference electrode. In this research, the potential scanning rate was 0.2 mV/s, and the potential range was -0.310~0.24 V vs. SCE. The electrochemical impedance spectroscopy (EIS) was tested in the frequency range of 0.01~10^5 Hz. PARSTAT 4000 electrochemical workstation was used for testing. Due to the service environment of Ni-Si alloy, 7wt% H_2SO_4 solution was selected as the electrochemical corrosion medium and prepared by distilled water.

2 Results and Discussion

2.1 Microstructure characterization

Fig. 1a shows the microstructure of $Ni\text{-}Ni_3Si$ eutectic composite without annealing. Fig. 1b~1d show the microstructures of $Ni\text{-}Ni_3Si$ eutectic composites after annealing at 950 °C for 2, 3, and 4 h, respectively. The light phase is α-Ni phase, the black one is $Ni\text{-}Ni_3Si$ eutectic phase, and the gray phase is metastable phase $Ni_{31}Si_{12}$.

As shown in Fig. 1, there are some changes in metastable phase. The metastable phase $Ni_{31}Si_{12}$ accounts for 58% of the total phase of Ni-Si eutectic without annealing. After annealing at 950 °C for 2 h, the proportion of metastable phase decreases to 44.2%. With increasing the holding time to 3 and 4 h at same annealing temperature, the proportion of metastable phase is decreased to 42.9% and 40.8%, respectively. Obviously, the annealing temperature of 950 °C is not high enough to reduce the metastable phase effectively, because eutectoid reaction occurs, i. e., metastable phase forms, at 990 °C during the directional solidification. Therefore, the metastable phase cannot be transformed below 990 °C.

Fig. 2a~2c show the microstructures of $Ni\text{-}Ni_3Si$ eutectic

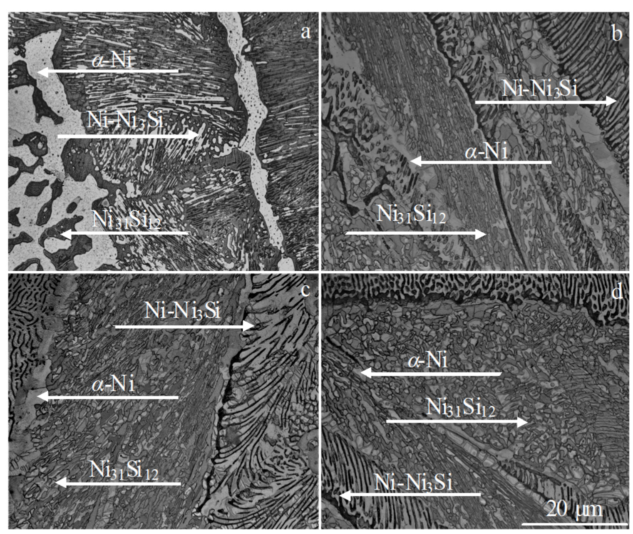

Fig.1 Microstructures of $Ni\text{-}Ni_3Si$ eutectic before (a) and after annealing at 950 °C for 2 h (b), 3 h (c), and 4 h (d)

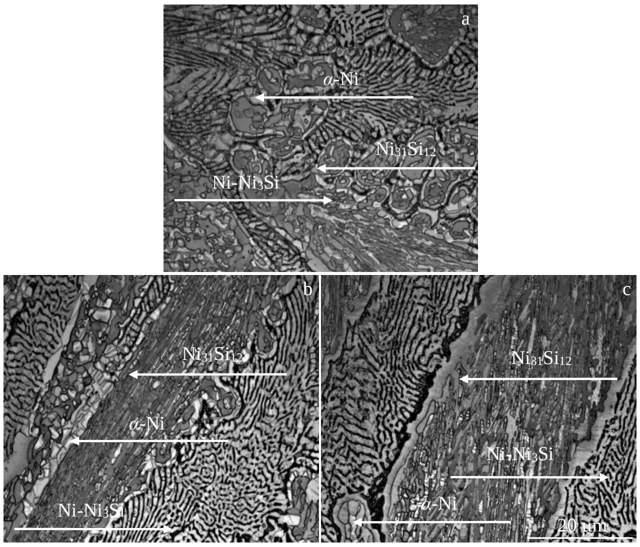

Fig.2 Microstructures of Ni-Ni_3Si eutectic after annealing at 1000 °C for 2 h (a), 3 h (b), and 4 h (c)

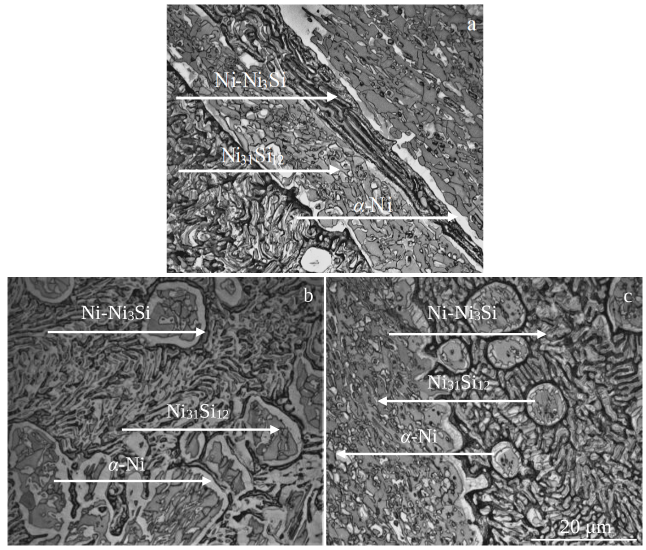

Fig.3 Microstructures of Ni-Ni_3Si eutectic after annealing at 1050 °C for 2 h (a), 3 h (b), and 4 h (c)

composites after annealing at 1000 °C for 2, 3, and 4 h, respectively. The amount of metastable phase changes obviously. After annealing at 1000 °C for 2 h, the proportion of metastable phase decreases to 30.6%. Compared with the results of annealing at 950 °C, the proportion of metastable phase is reduced to 33.7% and 35.6% with increasing the holding time to 3 and 4 h at 1000 °C, respectively. The metastable phase content generally shows a decrease trend due to the transformation of metastable phase $Ni_{31}Si_{12}$ into Ni_3Si phase. However, after annealing at 1000 °C for 3 and 4 h, the proportion of metastable phase is slightly higher, compared with the results of annealing for 2 h. This is because the eutectoid reaction, β_2-Ni_3Si→β_1-Ni_3Si+γ, occurs at 990 °C and it is reversible. When the holding time is too long, the metastable phases $Ni_{31}Si_{12}$ are gathered again, and the amount of metastable phase increases slightly.

Fig. 3a~3c show the microstructures of Ni-Ni_3Si eutectic composites after annealing at 1050 °C for 2, 3, and 4 h, respectively. The amount of metastable phase changes obviously. The proportion of metastable phase reduces to 31.8%, 28.6%, and 18.9% after annealing at 1050 °C for 2, 3, and 4 h, respectively. This phenomenon can be explained by the following reasons. Firstly, the furnace cooling after heat preservation produces non-equilibrium solidification during the slow cooling in this experiment. The transition processes from unstable phase to stable phase and from metastable phase to stable phase are not completely irreversible. In the competitive growth process between stable phase and metastable phase, it is necessary to overcome not only their interface energies, but also the strain energies due to the specific volume difference. The required energy is higher, so metastable phase cannot be completely transformed[15]. Secondly, according to the Ni-Si binary phase diagram, no matter which reaction is reversible, the eutectoid reaction, β_2-Ni_3Si→β_1-Ni_3Si+γ, occurs at 990 °C, and the metastable phase $Ni_{31}Si_{12}$ are gathered again. This is also an important reason why metastable phase cannot be completely eliminated. Thirdly, according to the Ni-Si phase diagram, the β_2-Ni_3Si phase decomposes into metastable phase when the temperature decreases to 1050 °C during the furnace cooling. Finally, under the synergistic effect of strong thermalmass disturbance of melt and curvature effect, the primary metastable phase is remelted and broken, and the intense energy fluctuation breaks the metastable phase into irregular shapes[16].

Through Image-Pro-Plus software quantitative analysis of microstructure, the amount of metastable phase in Ni-Si eutectic is listed in Table 1. It can be seen that the amount of metastable phase decreases obviously after annealing. The optimal heat treatment scheme is 1050 °C and holding time of 4 h, which results in the amount of metastable phase of 18.9%.

2.2 Electrochemical result

Fig.4 shows the potentiodynamic polarization curves of Ni-Si eutectic composites after different annealing processes in 7wt% H_2SO_4 solution. It can be seen that the self-corrosion potential of annealed specimens moves along the positive potential direction, compared with that of the untreated specimens. The more positive the self-corrosion potential, the more serious the impediment to the anodic reaction process, and the slower the corrosion rate. When the electrode potential increases to 0.7 V vs. SCE, the potential continues to increase,

Table 1 Amount of metastable phase at different annealing temperatures and holding time (%)

Holding time/h	950 °C	1000 °C	1050 °C
2	44.2	30.6	31.8
3	42.9	33.7	28.6
4	40.8	35.6	18.9

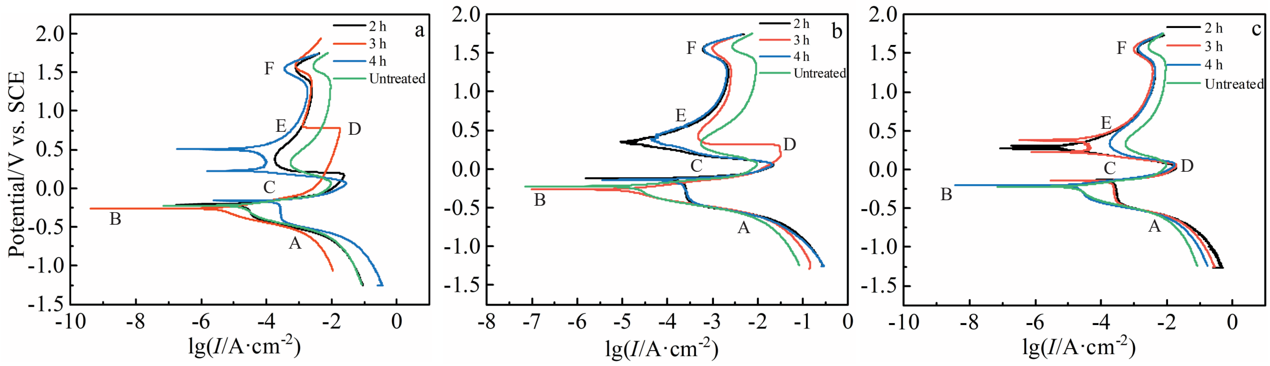

Fig.4 Potentiodynamic polarization curves of Ni-Si eutectic composites annealed at 950 °C (a), 1000 °C (b), and 1050 °C (c)

and the current density (I) remains basically unchanged in the anodic passivation zone. In this process, SiO_2 forms on the surface, and the passivation film prevents the specimen from reacting with H_2SO_4 solution and hinders the further corrosion.

As shown in Fig.4a, the AB section of polarization curve is the active dissolution zone. The reaction of anodic polarization is $Si\text{-}4e^- \rightarrow Si^{4+}$, which basically obeys the Tafel's Law. The dissolution rate of the anode gradually increases as the potential becomes positive. During dissolution process, the critical passivation current density of Ni is small, and the concentration of Ni^{2+} continuously decreases, making the alloy difficult to passivate. The anode current density of Si at the same potential is relatively large, and the product of the anodized film is mainly SiO_2. So it can be concluded that Si loses electrons. BC section is the passivation transition zone. When the potential passes B point, the specimen begins to enter the passivation stage, because SiO_2 passivation film forms during the first two stages and covers the specimen. The surface covered by passivation films leads to the decrease of the dissolution rate, and then specimen enters the passivation region. CD section is the stable passivation region where the current density hardly changes with the change of potential. In DE section, the current density changes obviously again, indicating that it is the over-passivation zone. This is due to the following two reasons: (1) the mechanical damage of the passivation film; (2) the hydrogen evolution reaction $H^+ + 2e^- \rightarrow H_2$. The passive film of metal is destroyed by hydrogen as a reducing gas. EF section returns to a stable passivation region. In the whole polarization process, the stability and instability states of the system is a dynamic process.

The highest self-corrosion potential, the smallest self-corrosion current density, and the optimal corrosion resistance were obtained under the condition of annealing temperature of 1050 °C and holding time of 4 h, indicating that the content and distribution of metastable phase have a certain influence on the corrosion rate. The lower content of metastable phase improves the corrosion resistance of Ni-Si eutectic.

Fig. 5 shows the Nyquist diagrams of Ni-Si eutectic composites after annealing at 950, 1000, and 1050 °C for 2, 3, and 4 h. It can be observed that the impedance spectra have similar changes under different annealing processes. The largest radius of capacitive arc is obtained when the annealing temperature and holding time is 1050 °C and 4 h, respectively. The electrochemical corrosion resistance is increased with decreasing the content of metastable phase, which is attributed to the transformation from metastable phase $Ni_{31}Si_{12}$ to stable Ni_3Si phase. The resistance of charge transfer between Ni-Si eutectic and solution increases. It is proved that the corrosion resistance of Ni-Si eutectic is related to the content of metastable phase at high solidification rate.

Table 2 shows the equivalent circuit parameters of Ni-Si eutectic composites before and after heat treatment in 7wt% H_2SO_4 solution. Fig. 6 is equivalent circuit diagram of Ni-Si eutectic composites in 7wt% H_2SO_4 solution. R_s is the solution

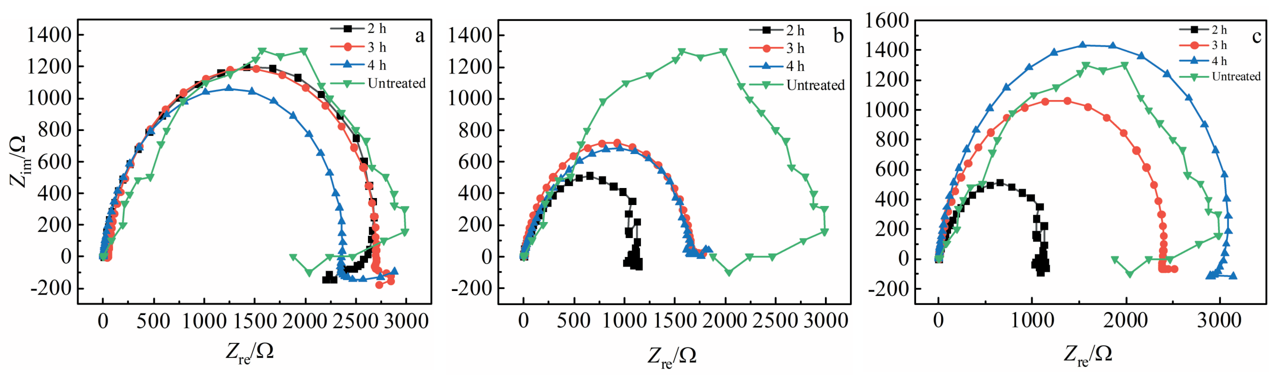

Fig.5 Nyquist diagrams of Ni-Si eutectic composites annealed at 950 °C (a), 1000 °C (b), and 1050 °C (c)

Table 2 Equivalent circuit parameters of Ni-Si eutectic composites before and after heat treatment in 7wt% H_2SO_4 solution

Annealing condition	R_s/ $\Omega\cdot cm^2$	Q/ $\times10^{-5}$ $F\cdot cm^{-2}$	n	R_{ct}/ $\times10^3$ $\Omega\cdot cm^2$
Untreated	1.615	3.916	0.8902	1.048
950 °C-2 h	1.638	2.480	0.9071	2.607
950 °C-3 h	1.643	1.938	0.9202	2.700
950 °C-4 h	2.628	2.705	0.9257	2.418
1000 °C-2 h	1.627	4.403	0.8801	1.122
1000 °C-3 h	2.026	3.549	0.8828	1.698
1000 °C-4 h	1.988	6.377	0.8350	1.702
1050 °C-2 h	1.530	3.868	0.8728	1.237
1050 °C-3 h	1.771	2.453	0.9229	2.417
1050 °C-4 h	2.759	1.755	0.9339	3.061

resistance, R_{ct} is the electrode resistance, Q is electrode capacitance, and n is a correlation coefficient of Q. In general, n is between −1~1, indicating the degree of dispersion effect. The closer the value of n to 1, the less the occurance probability of pitting corrosion. The larger the capacitance arc radius in high frequency region, the stronger the corrosion resistance of the material. It can be concluded that the majority of metastable phase $Ni_{31}Si_{12}$ is transformed into Ni_3Si by heat treatment. Ni-Ni_3Si eutectic effectively prevents the occurrence of corrosion. According to the data in Table 2, it can be clearly seen that the electrode resistance R_{ct} is the largest, the corrosion resistance is the highest, n is closest to 1, and the occurance possibility of pitting corrosion is the smallest when the annealing temperature and holding time is 1050 °C and 4 h, respectively, which is consistent with the polarization curve results.

Fig. 7 shows the corrosion surface morphologies of the annealed Ni-Ni_3Si eutectic composites after electrochemical corrosion in 7wt% H_2SO_4 solution. Corrosion pits can be observed in the matrix region, while no corrosion pits can be found in the Ni-Ni_3Si eutectic region. This phenomenon indicates that the corrosion mainly occurs in the matrix region. The spall of corrosion film is decreased with the increase of annealing temperature. The passive property and corrosion resistance of Ni-Si eutectic are mainly ascribed to the eutectic microstructure, because the corrosion occurs easily in metastable phase. After heat treatment, the homogenous structure is generated and corrosion resistance is improved due to the lower content of metastable phase. Meanwhile, the micropores cannot be formed on the surface owing to the unique eutectic structure of Ni-Ni_3Si, thereby effectively preventing pitting corrosion. For Ni-Si eutectic without annealing, the high content of metastable phase causes the constitutional segregation and an uneven structure, resulting in the generation of small holes on metal surface, which accelerates the corrosion pit evolution. This is the main reason for the instability and low corrosion resistance of composite with high content of metastable phase.

In order to determine the phase composition and phase distribution of Ni-Si eutectic composites after electrochemical corrosion, the EDAXXM2-60S spectrometer was adopted to detect the different phases in the specimens. The EDS mapping of element O, Ni, Si for Ni-Si eutectic zone is shown in Fig. 8. The EDS analysis result of Ni-Si eutectic zone is

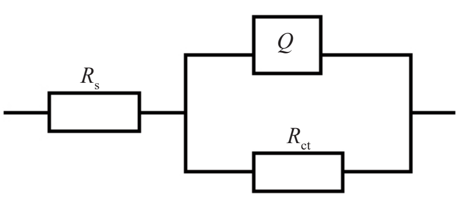

Fig.6 Equivalent circuit diagram of annealed Ni-Si eutectic composites in 7wt% H_2SO_4 solution

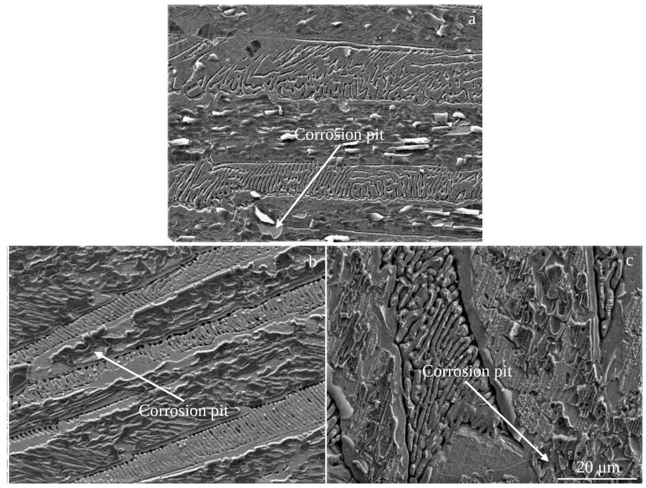

Fig.7 Corrosion surface morphologies of Ni-Si eutectic composites annealed at 950 °C (a), 1000 °C (b), and 1050 °C (c) in 7wt% H_2SO_4 solution

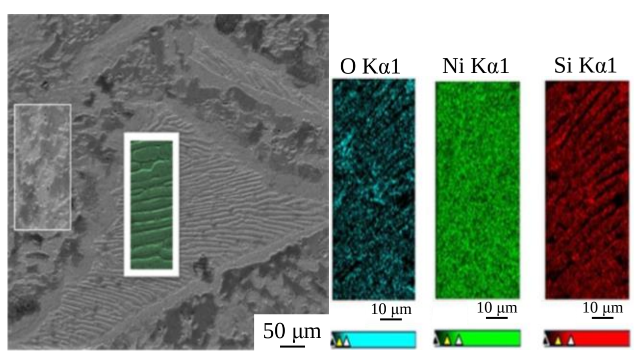

Fig.8 EDS element mapping of Ni-Si eutectic zone of annealed Ni-Si eutectic composite in 7wt% H_2SO_4 solution

Table 3 EDS results of Ni-Si eutectic composite (wt%)

Element	Content
O	10.22
Si	14.19
Ni	75.59

shown in Table 3. It is found that a compact SiO_2 film forms on the specimen surface to prevent further corrosion and improve the corrosion resistance of eutectic composites.

3 Conclusions

1) Metastable phase $Ni_{31}Si_{12}$ can be effectively transformed into stable Ni_3Si phase when the annealing temperature is 1050 °C and the holding time is 4 h.

2) Ni-Si eutectic composite has the highest self-corrosion potential, the smallest self-corrosion current density, and the strongest corrosion resistance after heat treatment of 1050 °C for 4 h. In addition, pitting corrosion mainly occurs in the matrix area rather than the eutectic area.

References

1 James S J, Venkatesan K, Kuppan P *et al*. *Procedia Engineering*[J], 2014, 97: 1018

2 Czél G, Jalalvand M, Wisnom M R. *Composite Structures*[J], 2016, 143: 362

3 Wu Zhifang, Liu Chao, Zhou Fan. *Powder Metallurgy Industry*[J], 2016, 26(2): 58 (in Chinese)

4 Palm M, Engberding N, Stein F *et al*. *Acta Materialia*[J], 2012, 60(8): 3559

5 Li Mingjun, Xue Yufang, Song Guangsheng. *Acta Metallurgica Sinica*[J], 1999, 35(5): 517 (in Chinese)

6 Yang Changlin. *Thesis for Master*[D]. Xi'an: Northwestern Polytechnical University, 2006 (in Chinese)

7 Wang Jing, Cao Chongde, Zeng Xiang *et al*. *Foundry Technology*[J], 2011, 32(7): 943 (in Chinese)

8 Hsu T Y. *Heat Treatment*[J], 2008, 23(2): 1

9 Lima L O R, Jacumasso S C, Martins J P *et al*. *Advanced Materials Research*[J], 2014, 891-892: 1111

10 Liu Meiying, Shan Nannan, Chen Linlin *et al*. *Applied Surface Science*[J], 2012, 258(20): 7922

11 Davies R G. *Metallurgical Transactions A*[J], 1978, 9(5): 671

12 Wu Yuanting, Li Menglong, Wang Xiufeng *et al*. *Advanced Manufacturing Processes*[J], 2016, 32(5): 480

13 Cui C J, Zhang J, Wu K *et al*. *Physica B: Condensed Matter*[J], 2012, 407(17): 3566

14 Dutra A T, Milenkovic S, Kiminami C S *et al*. *Journal of Alloys and Compounds*[J], 2004, 381(1-2): 40

15 Herlach D M, Feuerbacher B. *Advances in Space Research*[J], 1991, 11(7): 255

16 Li J F, Liu Y C, Lu Y L *et al*. *Journal of Crystal Growth*[J], 1998, 192(3): 462

亚稳相对定向凝固Ni-Si共晶腐蚀行为的影响

崔春娟[1,4]，刘　薇[1]，邓　力[1]，王松苑[1]，苏海军[2]，芦　禹[3]

(1. 西安建筑科技大学 冶金工程学院，陕西 西安 710055)

(2. 西北工业大学 凝固技术国家重点实验室，陕西 西安 710072)

(3. 伯明翰大学 冶金与材料学院，英国 埃德巴斯顿 B15 2TT)

(4. 陕西省冶金工程技术研究中心，陕西 西安 710055)

摘　要：采用改进的Bridgman定向凝固技术制备了凝固速率为25 μm/s的Ni-Si共晶复合材料。由于在凝固过程中不可避免地会产生亚稳相$Ni_{31}Si_{12}$，采用退火工艺以减少亚稳相的含量，并利用电化学阻抗谱和电位动力学极化技术分析了材料在25 ℃、7%（质量分数）H_2SO_4溶液中的耐腐蚀性，并进行了等效电路分析。结果表明，退火处理（1050 ℃、4 h）改善了亚稳相$Ni_{31}Si_{12}$的含量和分布，退火后Ni-Si共晶的钝化性能和耐腐蚀性提升。亚稳相的含量越少，耐腐蚀性能越强。

关键词：Bridgman定向凝固；Ni-Si共晶复合材料；亚稳相；腐蚀行为；电化学

作者简介：崔春娟，女，1972年生，博士，教授，西安建筑科技大学冶金工程学院，陕西 西安 710055，电话：029-82202923，E-mail：cuichunjuan@xauat.edu.cn